ELSEVIER

Biophysical Chemistry 75 (1998) 163–176

Biophysical Chemistry

Self assembly driven by hydrophobic interactions at alkanethiol monolayers: mechanism of formation of hybrid bilayer membranes

J.B. Hubbard[a,*], V. Silin[b], A.L. Plant[a]

[a] *Biotechnology Division, National Institute of Standards and Technology, Gaithersburg, MD 20899, USA*
[b] *Department of Chemistry, Georgetown University, Washington, DC 20057, USA*

Received 13 July 1998; accepted 29 July 1998

Abstract

The mechanism for the formation of biomimetic model cell membranes consisting of bilayers composed of alkanethiols and phospholipids was probed with a kinetic study using surface plasmon resonance. The kinetics of formation of a monolayer of phospholipid from vesicles in solution onto a hydrophobic alkanethiol monolayer is described by a model that takes into account the lipid concentration, diffusion, and a surface reorganization rate constant. Monomer phospholipid apparently does not play a direct role in determining the kinetics of bilayer formation. Expressions for the limiting cases of this model describe the behavior of two distinct vesicle concentration conditions. At high concentrations of lipid vesicles the formation of the bilayer appears to be limited by the diffusion of vesicles to the surface; at lower concentrations of vesicles, the rate-limiting step is apparently the surface reorganization of lipid. This kinetic model can also be used to describe the formation of a biomimetic bilayer from an alkanethiol monolayer and cell membranes.

Keywords: Alkanethiols; Phospholipids; Bilayers; Kinetic study; Surface plasmon resonance

1. Introduction

Self-assembly can control the modification of surfaces with precision in molecular structure and chemical composition. Surfaces modified by self-assembly have applications in sensors, diagnostics, chemical processing, and biomimetic materials, where they may incorporate features such as molecular recognition and enzymatic activity. Understanding the forces that direct self-assembly of biological molecules in predictable arrangements will aid the development of such applications.

This is one in a series of studies whose ultimate goal is the development of methodology for producing and analyzing well-characterized, robust biomimetic surfaces which form by molecular self-assembly. The focus of this study is a mimic of biological membranes that is formed by the interaction between two self-assembling systems:

* Corresponding author.

0301-4622/98/$ - see front matter
PII S0301-4622(98)00199-9

phospholipid amphiphiles that associate into bilayer vesicles in water, and monolayers of alkanethiols on metal surfaces. The resulting structure is a hybrid bilayer membrane (HBM), which is composed of a layer of alkanethiol and a layer of phospholipid. This model system is being developed as a tool for the study of membrane protein structure and function, and for studies of biochemical processes which require a cellular membrane environment.

The spontaneous formation of a planar lipid bilayer by the addition of vesicles to a supported lipid monolayer was first reported by Kalb et al. [1]. Using alkanethiol monolayers as the hydrophobic surfaces, we have formed and characterized the resulting hybrid bilayer membranes by impedance spectroscopy [2], FTIR spectroscopy [3] and neutron reflectivity [4]. Alkanethiols have advantages over other hydrophobic monolayers in that they interact strongly with the gold surface and form complete and rugged monolayers of well-packed alkane molecules. This reduces some of the possible variability that can complicate studies that use lipid monolayers that are weakly associated with surfaces.

Here we are attempting to elucidate the physico-chemical mechanisms by which these bilayers form. A depiction of the events considered in the formation of a HBM is shown in Fig. 1. The process of HBM formation is an example of the effect of interfacial free energy on molecular reorganization at a surface. Phospholipids have a small aqueous partition coefficient; in solution, phospholipid molecules exist primarily as suspended long-lived metastable lipid vesicles. When exposed to the hydrophobic alkanethiol monolayer surface, phospholipid molecules from the vesicle solution spontaneously add a single molecular layer to the surface. In the equilibrium structure the polar headgroups of the lipids face away from the support and into the aqueous phase, and the alkane chains of the thiol and the lipid are associated with one another and sequestered from the water phase. The mechanism of bilayer formation might be expected to influence the resulting composition of the lipid bilayer. For example, if the formation of the bilayer occurs by addition of individual phospholipid molecules to the surface,

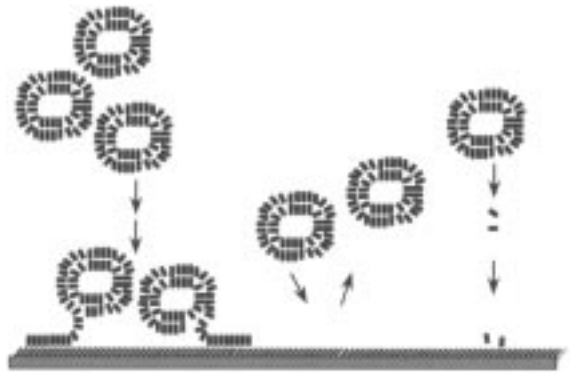

Fig. 1. Three processes by which phospholipid molecules might add to a hydrophobic monolayer are considered. From left to right: diffusion of lipid vesicles to the hydrophobic surface is rate-limiting while reorganization of lipid at the surface is fast; fusion of vesicles with the surface is inhibited so that surface reorganization is slow, resulting in the appearance of a partially reflecting boundary as vesicles return to the bulk solution; phospholipid monomers, present at a very low concentration, diffuse to the surface as the layer assembles one molecule at a time.

the composition may be significantly different than if a cooperative deposition of molecules comprising the vesicle lamellae is responsible for bilayer formation. For the purpose of reassembling a complex biomimetic membrane, it would also be of interest to know if components from both lamellae of phospholipid vesicles contribute lipid to the surface, and if the inside/outside relationship of vesicle lamellae is retained in HBMs.

Lowering the free energy of the hydrophobic surface by bilayer formation may be accompanied by a free energy penalty associated with vesicle disruption. Understanding the mechanism by which vesicles contribute lipid to the hydrophobic interface may provide insight into how to design the interface and/or the vesicles to make the process even more thermodynamically favorable. We are addressing this issue using kinetic data generated by surface plasmon resonance (SPR) combined with a theoretical modeling effort which incorporates the effects of mass transport by diffusion, surface reorganization dynamics, and adsorption saturation. The key observation in SPR is the time course of the build up of the lipid surface layer until saturation is apparently reached at monolayer coverage. Several recent

reports on similar experimental systems [5–7] qualitatively support the data reported here. However, to our knowledge, there have as yet been no meaningful kinetic models put forth to describe the details of the process.

The modeling task is to rationalize and ultimately to predict this growth of surface coverage in terms of fundamental physical parameters such as diffusion coefficients, available (unsaturated) surface area, and surface reorganization rate constants. In particular, it is highly desirable to construct a physical model which enables us to deduce the extent to which monolayer formation is controlled by kinetics (e.g. bulk diffusion) or thermodynamics (e.g. surface reorganization), and whether surface deposition of phospholipid molecules is due predominantly to the addition of lipid molecules as monomers, or is a cooperative process associated with lipid vesicles.

2. Materials and methods[1]

2.1. Lipid vesicles

Dimyristoylphosphatidyl choline (DMPC) was purchased from Avanti Polar Lipids, (Alabaster, AL). To prepare vesicles, 2 μmol of DMPC in chloroform were dried under a nitrogen stream and held under vacuum overnight. The lipid was then dissolved in 50 μl of isopropanol and injected with a Hamilton syringe into 1 ml of rapidly stirring buffer solution (5×10^{-2} mol/l sodium phosphate, pH 7.4). The concentration of phospholipid in this preparation was 2×10^{-3} mol/l, and subsequent dilutions were prepared from this sample. This procedure resulted in uniform vesicles with a diameter of ~ 0.1 μm as determined by quasielastic light scattering (QEL) measurements [8] on solutions of concentrations of 5×10^{-5} mol/l lipid and higher.

2.2. Red blood cell ghosts

Red blood cells were isolated from freshly drawn human blood. Preparation of ghosts for use in this study was described previously [9] and was based on the method of Steck and Kant [10]. The protein concentration of the ghost preparation was determined using the bicinchonic acid assay (Pierce Chemical Co., Rockford, IL). Ghosts were used at a protein concentration of ~ 0.1 mg/ml. The composition of RBC ghosts is $\sim 50\%$ protein, 43% lipid and 7% carbohydrate by dry weight [11]. QEL indicated a diffusion coefficient of 2×10^{-9} cm^2 s^{-1}, corresponding to a hydrodynamic radius of 1.58 μm.

2.3. Surface plasmon resonance

SPR has been widely used in recent studies of biochemical interactions at surfaces [12]. The characteristics of the SPR device, its calibration, the preparation of gold films on glass substrates, and the procedure of SPR measurements in flow have been described previously [13]. The optical components include a semiconductor laser (750 nm), a polarizer to create *p*-polarized light, a beam expander to increase beam size by approximately a factor of 10, a cylindrical lens to focus the laser beam on the sample with an angle distribution of $\sim 10°$, a glass prism, and a CCD detector with 512 pixels. An alkanethiol monolayer was formed from an ethanolic solution of either 1 mM dodecanethiol or hexadecanethiol onto a 45-nm-thick gold film deposited on a glass substrate. The glass/gold substrate was mounted as a component of the sample cell in optical contact with the glass prism. The cell volume was 1 ml, and the surface area of the gold-coated sample was 0.32 cm^2. These elements were mounted on a rotating optical table with an angle resolution of 0.001 degrees. The prism provided for the possibility of changing the laser beam incidence angle while simultaneously keeping the reflection beam in the same position on the CCD detector. Fast linearized least-squares fitting of the data to a Gaussian function allowed determination of the SPR minimum position (in pixels) and the SPR line width. The time to measure one point was ~ 10 s. The measured resolution of the SPR device was ~ 0.1 pixels of the CCD. The measurements reported here were performed un-

[1] The identification of commercial products does not constitute endorsement by NIST.

der non-flowing conditions. A stable baseline was ensured by adding buffer to the cell and collecting data for ~30 min prior to removing the buffer solution and replacing it with solution containing vesicles or red blood cell ghosts. The time required to exchange solutions was less than 5 s. All measurements were carried out at room temperature (24°C). Experimental data were corrected for the refractive index change observed when buffer was replaced with vesicle solution. The presence of isopropanol in the vesicle solution significantly contributed to this change in refractive index. Since the buffer solution in the cell was replaced with vesicle solution within 3 to 5 s, the change in refractive index solely due the difference of the solutions was easily subtracted from the change due to the bilayer formation process, which occurred over much longer times.

The SPR response was calibrated using a solution of known refractive index as described previously [12]. From this it was calculated that for a layer with a refractive index of 1.45, a 1-pixel shift in SPR minimum corresponded to a thickness change of 0.6 Å.

2.4. Data analysis

Fitting of kinetic data was performed using Sigma Plot (SPSS Inc., Chicago, IL). Selected data were also fit to a logarithmic form of Eq. (1) using CMLIB (NIST, Gaithersburg, MD). Both analyses yielded the same results.

3. Results and discussion

The experimental results for addition of DMPC to the hydrophobic alkanethiol surface are presented in Fig. 2. The data (dotted lines) show that the time-dependence for increase in surface layer thickness is strongly dependent on the concentration of phospholipid vesicles in the solution. For this study, experiments were conducted under static, non-flowing, conditions. The kinetics of phospholipid addition to the alkanethiol layer are

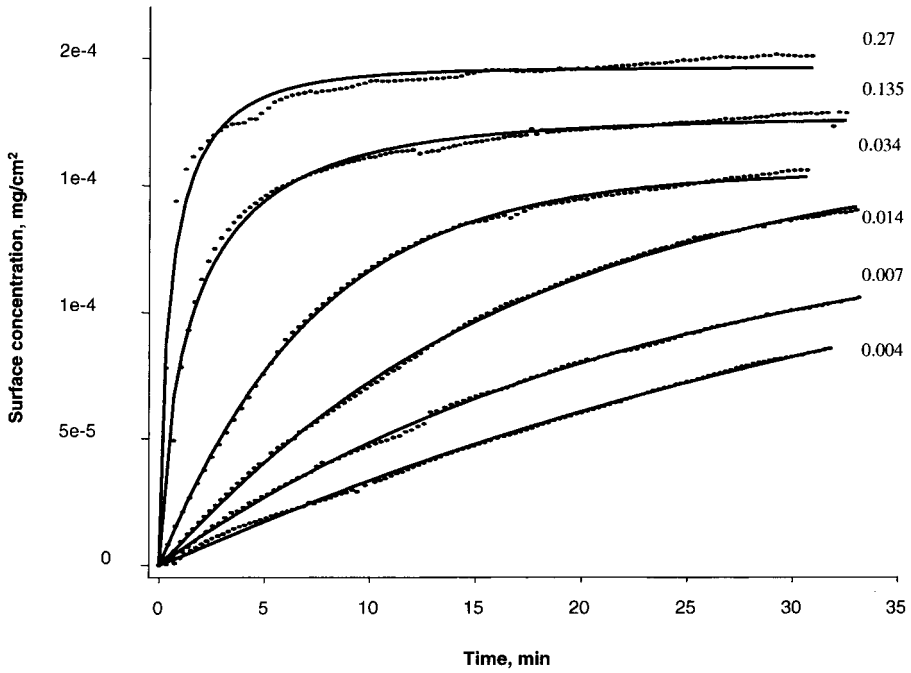

Fig. 2. Bilayer formation kinetics as measured using SPR. Phospholipid vesicles are added to the cell at $t = 0$. Dots represent experimental points; solid lines were calculated using global model, Eq. (1). Bulk vesicle concentrations were: 0.004, 0.007, 0.014, 0.034, 0.135 and 0.27 mg/ml phospholipid.

generally more rapid under conditions of continuous flow where the rate of mass transport of vesicles to the surface is enhanced, but the data are more difficult to model than under the conditions used in this study. Experiments in flow were used to confirm the final monolayer thickness of about 22 Å that was observed for the thickness of the phospholipid layer after saturation.

Initial attempts to fit the data involved consideration of previously published approaches to analysis of similar kinetic phenomena. Purely empirical approaches to surface adsorption of proteins [14] and polymers [15] have been described. Combinations of simple exponentials with stretched exponentials yielded fits to our data that were quite good, but required the introduction of a number of adjustable parameters of no apparent physical significance. We also considered a random sequential adsorption model in which the rate of collision between vesicles and the surface is the only kinetic parameter. Such a model predicts an algebraic approach to saturation, and results in poor fits to our data.

A key observation in our SPR data is the continuous increase in the thickness of the surface lipid layer with time until saturation is apparently reached at monolayer coverage. The model presented here is intended to rationalize the kinetics of this process in the context of bulk diffusion coupled to surface reorganization. We consider the following probable sequence of events: diffusion of vesicles and/or lipid monomer molecules to the surface where they are either repelled or retained, followed by adsorption and/or reorganization at the surface, and with time, saturation of the surface with a monolayer of lipid.

3.1. Models and data fitting

The mathematical form of the model expresses the time-dependent surface concentration in terms of the maximum surface coverage of phospholipid, the bulk concentration of an adsorbing species, the bulk diffusion of an adsorbing species, and a surface reorganization rate constant:

$$\Gamma(t) = \Gamma_m \left\{ 1 - \exp \frac{-KC_0}{\Gamma_m} \left[\frac{D}{K^2} \left(\exp\left[\frac{K^2 t}{D} \right] \cdot erfc\left[\left(\frac{K^2 t}{D} \right)^{1/2} \right] - 1 \right) + \frac{2}{K} \left(\frac{Dt}{\pi} \right)^{1/2} \right] \right\} \quad (1)$$

where *erfc* indicates the complementary error function [16].

To derive Eq. (1) we assume Fickian diffusion to an imperfectly absorbing (partially reflecting) surface whose active sites are blocked by previously adsorbed lipid:

$$\Gamma(t) = \int_0^t d\tau \left(1 - \frac{\Gamma(\tau)}{\Gamma_m} \right) F_D(\tau) \quad (2)$$

where the time-dependent surface concentration (in mg cm^{-2}), $\Gamma(t)$, is expressed in terms of Γ_m, the maximum surface coverage of phospholipid, and

$$\left(1 - \frac{\Gamma(\tau)}{\Gamma_m} \right)$$

is the fraction of the surface which is not covered at time τ.

The diffusive flux to the surface, F_D, is given by [17]

$$F_D = KC_0 \exp\left(\frac{K^2 t}{D} \right) erfc\left(\frac{K}{D^{1/2}} t^{1/2} \right) \quad (3)$$

where C_0 is bulk concentration of absorbing species (vesicles or monomer phospholipid), D is the bulk diffusion coefficient of vesicles or monomer phospholipid, and the surface reorganization rate constant (or inverse reflection coefficient) is K (in cm s^{-1}). In this model, the kinetic constant, K, reflects a surface reaction with linear dimensions of cm s^{-1}. We speculate that this constant may be the square root of the product of a surface diffusion constant, with units of cm^2 s^{-1}, and reorganization constant, with units of s^{-1}. Eq. (3) gives the diffusive flux to an imperfectly absorbing surface with the mixed boundary condition

$$D\frac{\partial C}{\partial x}|\text{surface} = KC|\text{surface} \quad (4)$$

This expression sets the diffusive surface flux proportional to the surface concentration. We emphasize that Eq. (1) is the exact solution to the integral Eq. (2) with F_D given by Eq. (3) which satisfies the boundary conditions

$$\Gamma_0 = 0, \quad \Gamma_\infty = \Gamma_m \quad (5)$$

that correspond to zero initial surface coverage, and surface saturation at monolayer coverage which is approached at infinite time. Note that $\Gamma(t)$ exhibits a smooth monotonic approach to saturation, which is in accord with our experimental data.

To the best of our knowledge, Eq. (1) has not previously appeared in the literature, but two limiting cases of this expression have been extensively used to correlate polymer [15,18,19] and protein surface adsorption data [19,20]. At the limit of large values of K^2/D, the expression yields a stretched exponential with index 1/2:

$$\Gamma(t) = \Gamma_m\left[1 - \exp\left(-\frac{2C_0}{\Gamma_m}\left(\frac{Dt}{\pi}\right)^{1/2}\right)\right] \quad (6)$$

At the limit of small values of K^2/D, the approach to saturation is a simple exponential:

$$\Gamma(t) = \Gamma_m\left[1 - \exp\left(-\frac{KC_0 t}{\Gamma_m}\right)\right] \quad (7)$$

The former case is usually designated as diffusion dominated adsorption kinetics whereas the latter case defines a regime controlled by thermodynamic or surface kinetic effects [15].

The rate constant K characterizes the influence of surface reorganization kinetics on the surface concentration of lipid. We emphasize that K refers not only to the surface adsorption of intact vesicles, but also incorporates the vesicle disruption process and the surface migration dynamics of lipid monomer. K therefore designates an entire set of quite complex surface kinetic processes. Large values of K ($K^2/D \gg 1$) correspond to instantaneous surface kinetics (compared to diffusion) and therefore perfect adsorption at available surface sites. Small values of K imply that bulk material is partially reflected or repelled by the active surface, and that surface kinetic processes are slow relative to diffusion.

We fit the data using non-linear least squares analysis to the general expression and to the limiting cases. Parameters are based on known quantities or reasonable estimates. For example, the concentration of lipid was controlled, and the concentration of lipid present in the form of solubilized monomer lipid (equivalent to the critical micelle concentration) was calculated [21]. These parameters were held constant during fitting. The bulk diffusion coefficient of lipid vesicles was directly measured by dynamic light scattering. The diffusion coefficient for phospholipid monomer was estimated based on an assumption of proportionality of molecular radius r and diffusion coefficient: $D \sim 6\pi\eta_s r^{-1}$ [8]. Values for these parameters were confined during fitting to within two orders of magnitude of the initial estimates. The number of phospholipid molecules at the surface at saturation, Γ_m, was allowed to float, although an estimate for Γ_m was based on the known headgroup area of DMPC [22], and this value provided an initial guess. The only other fully adjustable parameter for fitting was the surface reorganization rate constant, K.

For this analysis, we made no assumptions about the specific nature of any surface reorganization process, but combined all unknown kinetic quantities into the single constant, K. Table 1 shows the initial values for parameters used for non-linear least squares fitting of the experimental data to the models.

3.2. Fitting results for the contribution from vesicles

The results of fitting the kinetic data to Eq. (1) are shown in Fig. 2 and Table 2 for the case where C equals the concentration of lipid in vesicles. As can be seen by Fig. 2, the model described by Eq. (1) fits all the data sets well. The resulting fit parameters shown in Table 2 indicate that the model provides similar and reasonable estimates for Γ_m for all data sets. These values are consistent with a DMPC area per molecule of

Table 1
Initial values for parameters used for non-linear least squares fitting of the experimental data

C, concentration of lipid in the form of vesicles	0.27 mg ml^{-1} to 0.004 mg ml^{-1}
C, concentration of solvated lipid monomer[a]	6×10^{-6} mg ml^{-1}
D, diffusion coefficient for lipid vesicles[b]	5.0×10^{-8} cm^2 s^{-1}
D_1, diffusion coefficient for solvated lipid monomers[c]	2.5×10^{-6} cm^2 s^{-1}
Γ_{max}, PL maximum surface concentration[d]	2.3×10^{-4} mg cm^{-2}
D_h, diffusion coefficient for red blood cell ghosts[b]	2.0×10^{-9} cm^2 s^{-1}
Sample volume	1 ml

[a] The calculated CMC for DMPC [21,23].
[b] Experimentally determined by QEL.
[c] Estimated from $D \sim 6\pi\eta_s r^{-1}$ [8].
[d] Estimated assuming 50 Å^2 per DMPC headgroup [22].

50 Å^2, the area per DMPC headgroup below its phase transition temperature [22]. Variability in the magnitude of Γ_m may reflect less than complete ordering of the layer, particularly at smaller concentrations. Alternatively, it may be that it is simply more difficult to estimate Γ_m for the lower concentration data which correspond to relatively early times in the bilayer formation process. The results shown in Table 2 indicate that at the two highest concentrations of lipid in vesicles the diffusion coefficients are similar to that measured for vesicles in the bulk. For the four lowest concentrations of vesicles, the fitted curves are insensitive to D as is indicated by the large standard errors. The magnitude of these fitted values is similar to a diffusion coefficient for monomer phospholipid, but the large standard errors suggest that these values are not very meaningful. As will be shown, these data can be fit very well to a model that does not include D.

The estimates for K, the surface reorganization rate constant, are slightly lower for these concentrations than for the two highest concentrations. The data suggest that perhaps we are observing two apparent concentration regimes, one kinetically limited by vesicle diffusion, and another limited by vesicle reorganization.

To test this hypothesis, we applied the expressions for two limiting cases, the diffusion-limited regime corresponding to Eq. (6), and the thermodynamic or surface reorganization limit as described by Eq. (7). Fig. 3a and Table 3 show that the high concentration data fit well to the diffusion dominated adsorption limit as described by Eq. (6). In fact, this model is preferred for describing these high concentration data, since the fitted values for diffusion coefficients are more like the experimentally observed diffusion coefficient for vesicles. These results suggest that diffusion of lipid vesicles to the hydrophobic surface is largely responsible for the rate of phospholipid addition provided that the concentration of vesi-

Table 2
Calculated parameters from fitting experimental data to Eq. (1). Mean values are followed by standard errors associated with uncertainty in the fit. Table entries marked with '*' have high standard errors and are probably meaningless

Lipid concentration C, mg/ml	Surface coverage Γ_m, mg/cm^2	Apparent vesicle diffusion coefficient D, cm^2/s	Effective surface reorganization rate constant K, cm/s
0.004	$2.3 \times 10^{-4} \pm 3.6 \times 10^{-5}$	$2.0 \times 10^{-5*} \pm 2.2 \times 10^{-5}$	$1.6 \times 10^{-5} \pm 3.7 \times 10^{-7}$
0.007	$1.4 \times 10^{-4} \pm 3.3 \times 10^{-6}$	$6.8 \times 10^{-5*} \pm 1.4 \times 10^{-4}$	$1.5 \times 10^{-5} \pm 1.3 \times 10^{-8}$
0.013	$1.64 \times 10^{-4} \pm 1.0 \times 10^{-6}$	$2.3 \times 10^{-3*} \pm 1.0 \times 10^{-3}$	$1.3 \times 10^{-5} \pm 1.7 \times 10^{-7}$
0.034	$1.55 \times 10^{-4} \pm 3.3 \times 10^{-7}$	$8.0 \times 10^{-4*} \pm 4.0 \times 10^{-4}$	$1.1 \times 10^{-5} \pm 1.3 \times 10^{-8}$
0.135	$1.77 \times 10^{-4} \pm 5.0 \times 10^{-8}$	$2.0 \times 10^{-8} \pm 1.3 \times 10^{-9}$	$3.2 \times 10^{-5} \pm 3.3 \times 10^{-6}$
0.27	$1.96 \times 10^{-4} \pm 5.0 \times 10^{-8}$	$1.3 \times 10^{-8} \pm 1.3 \times 10^{-9}$	$7.2 \times 10^{-5} \pm 1.5 \times 10^{-6}$

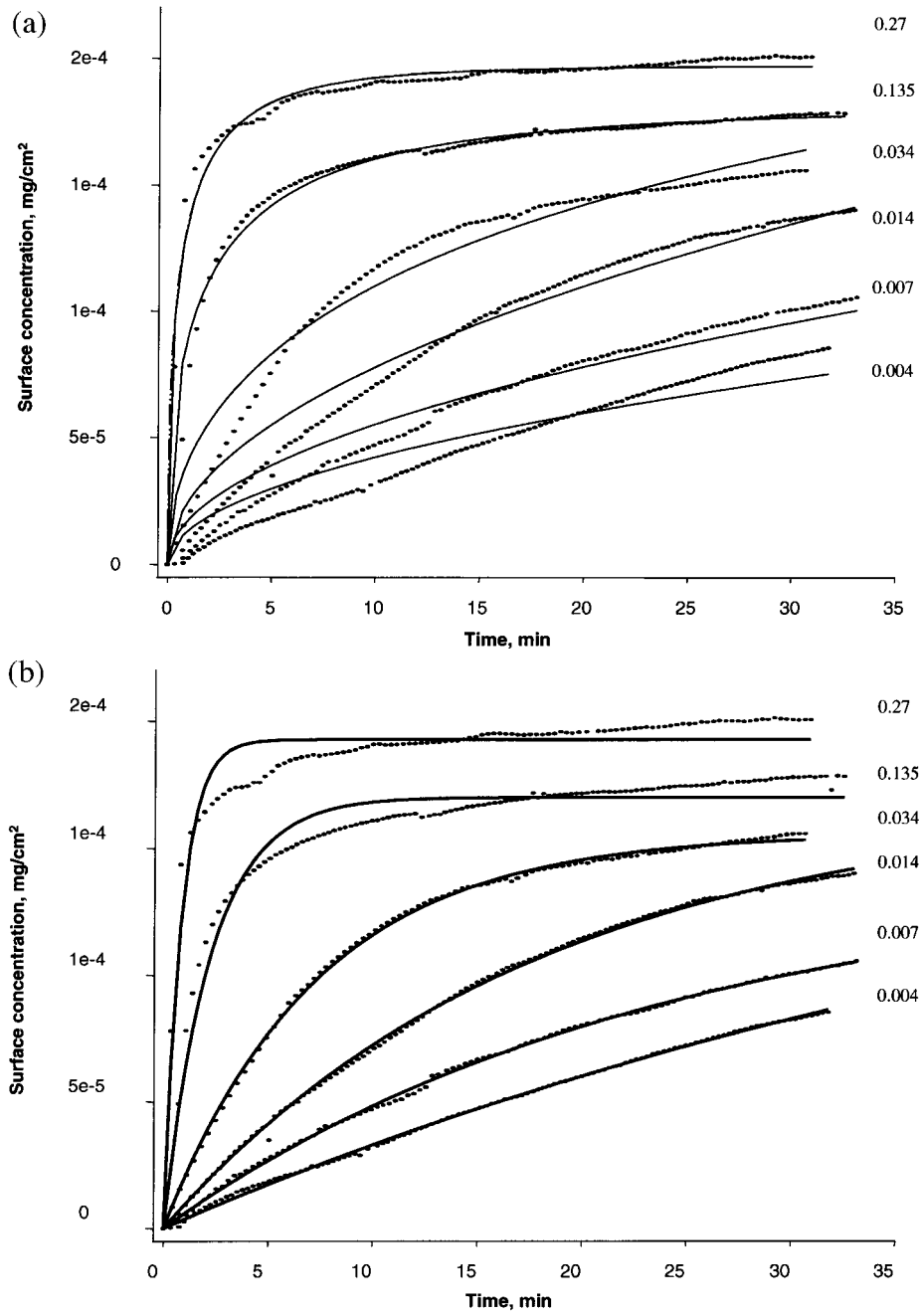

Fig. 3. (a) The same data as shown in Fig. 2, but solid lines are calculated using Eq. (6), the diffusion limited case. (b) The same data as shown in Fig. 2, but solid lines are calculated using Eq. (7), the surface reorganization limited case.

cles is high. The fact that the reorganization parameter, K, is not needed to fit these data indicate that K is effectively infinite in this case, and the values for K that are reported in Table 2 for the two highest concentrations apparently have no physical meaning.

Table 3
Calculated parameters from fitting experimental data to Eq. (6), the diffusion limit

Lipid concentration, C_0 (mg/ml)	Surface coverage, Γ_m (mg/cm^2)	Apparent vesicle diffusion coefficient, D (cm^2/s)
0.135	$1.81 \times 10^{-4} \pm 6.9 \times 10^{-7}$	$11.0 \times 10^{-8} \pm 3 \times 10^{-10}$
0.27	$1.97 \times 10^{-4} \pm 4.9 \times 10^{-7}$	$9.5 \times 10^{-8} \pm 3 \times 10^{-10}$

As seen in Fig. 3a, Eq. (6) did a poor job of describing the data when the concentration of vesicles is low. Since a kinetic process in addition to diffusion seemed likely to be important at least at low vesicle concentrations, we next consider the limit where the reorganization of molecules at the surface is the rate-limiting step in the process of HBM formation. The SPR kinetic data associated with the four lower concentrations of lipid vesicles were well fit by Eq. (7), the thermodynamic limit, as shown in Fig. 3b and Table 4. In contrast, the high concentration data were not described well by this thermodynamic limit (Fig. 3b).

This result indicates that at lower vesicle concentrations the rate of vesicle diffusion to the surface is not independent of a secondary event at the surface. At high concentrations of lipid, the dependence on the diffusion coefficient of vesicles indicates the development of a time-dependent concentration gradient profile at the surface. Processes occurring at the surface apparently are fast relative to diffusion. At the lower lipid concentrations, surface events are slow, and there is no evidence of the process being limited by diffusion of vesicles. Such surface events could include the non-productive association of lipid vesicles with the surface, i.e. approach of vesicles that fail to reorganize at the surface.

Values in Table 4 are very similar to the corresponding values in Table 2. Using either Eq. (1) or Eq. (7), a kinetic constant of about 1.45×10^{-5} cm s^{-1} was calculated for the reorganization of vesicles at the surface when the concentration of vesicles was less than 0.2 mmol l^{-1} in total lipid. A reorganization process must be considered for the low concentration data in order to achieve a good fit. In contrast, the high concentration data can be fit without considering such a reorganization process. These results suggest that surface reorganization of lipid is more kinetically limiting under conditions of low vesicle concentration than under conditions of high vesicle concentration.

3.3. The role of phospholipid monomer

The critical micelle concentration (CMC) for DMPC can be calculated [21] to be $\sim 1 \times 10^{-11}$ mol/ml (6×10^{-6} mg/ml). As described by Smith and Tanford [23], once the CMC is reached, the free amphiphile concentration in equilibrium with vesicles is largely independent of the concentration of vesicles, especially when the aggregate structure is composed of large numbers of monomers. The hydrophobic surface area exposed to solution is ~ 0.32 cm^2, which can accommodate $\sim 1 \times 10^{-10}$ mol of phospholipid as a monolayer. Although the molar ratio of phospholipid as monomer compared to phospholipid in vesicles ranges from only 0.002% to a high of

Table 4
Calculated parameters from fitting experimental data to Eq. (7), the reorganization, or thermodynamic, limit

Lipid concentration, C_0 (mg/ml)	Surface coverage, Γ_m (mg/cm^2)	Effective surface reorganization rate constant, K (cm/s)
0.004	$1.9 \times 10^{-4} \pm 6.0 \times 10^{-8}$	$1.66 \times 10^{-5} \pm 7.5 \times 10^{-8}$
0.007	$1.4 \times 10^{-4} \pm 1.5\ 10^{-8}$	$1.45 \times 10^{-5} \pm 7.0 \times 10^{-8}$
0.013	$1.69 \times 10^{-4} \pm 1.0 \times 10^{-8}$	$1.2 \times 10^{-5} \pm 5.0 \times 10^{-8}$
0.034	$1.56 \times 10^{-4} \pm 5.0 \times 10^{-9}$	$1.05 \times 10^{-5} \pm 5.0 \times 10^{-8}$

0.15%, we might anticipate that free monomer could rapidly diffuse to and associate with this hydrophobic surface. In 1 ml of lipid vesicles, enough monomer lipid molecules are present to cover $\sim 10\%$ of the hydrophobic surface area. Furthermore, re-equilibration of phospholipid monomers from vesicles to the aqueous phase could continue to occur over the course of the experiment. Dissociation of monomer lipid is the rate-limiting step in the aqueous phase transfer of these molecules between hydrophobic compartments, and this process has a rate constant that can be calculated to be 0.16 min^{-1} for DMPC [24]. Within the timecourse of this measurement, we could expect that dissociation of monomer phospholipid into the bulk aqueous phase could contribute as much as 30% of the lipid needed to saturate the surface. The possible contribution of lipid monomer was considered explicitly with a two-component model.

The mathematical treatment that produced Eq. (1) can be easily generalized to deal with the diffusion and surface adsorption of a number of species that compete with some arbitrary affinity. Ignoring the saturation condition for a moment, the surface concentration of species i can be defined as

$$\Gamma_i'(t) = K_i C_i \left[\frac{D_i}{K_i^2} \left(\exp\left[\frac{K_i^2 t}{D_i} \right] \cdot erfc\left[\left(\frac{K_i^2 t}{D_i} \right)^{1/2} \right] - 1 \right) + \frac{2}{K_i} \left(\frac{D_i t}{\pi} \right)^{1/2} \right] \tag{8}$$

Under conditions where surface saturation can occur, the time-dependent surface concentration then takes the form

$$\Gamma(t) = \Gamma_m \left\{ 1 - \exp - \left(\frac{\sum_i \Gamma_i'(t)}{\Gamma_m} \right) \right\} \tag{9}$$

where the summation is over all species. For the case where both intact vesicles and phospholipid monomer are considered, we have

$$\Gamma(t) = \Gamma_m \left\{ 1 - \exp - \left(\frac{\Gamma_1'(t) + \Gamma_2'(t)}{\Gamma_m} \right) \right\} \tag{10}$$

where $\Gamma_1'(t)$ refers to vesicles and $\Gamma_2'(t)$ corresponds to monomer.

Because Eq. (10) contains two linearly dependent parameters, K_1 and K_2, we attempted to fit multiple data sets simultaneously to one set of parameters to improve the validity of the results. Simultaneous fitting of the four lowest vesicle concentrations was achieved, but attempts at simultaneous fitting of data for the two largest concentrations did not produce satisfactory fits and so these data were fit independently. Diffusion coefficients, D_1 and D_2, corresponding to vesicles and lipid monomer, and maximum surface concentration, Γ_m, were adjustable parameters, while the concentration of lipid as vesicles, C_1, and lipid as monomer, C_2, were kept constant. We found that the two-component model provided fits that matched the data as well as did the one component model. This was not unexpected since the number of fitted parameters increased.

Interestingly, fitting the data to this model provided no indication that lipid monomer plays a significant role in bilayer formation. The fitted parameters resembled those found for the one-component model, in that, for the low concentration data, D_1 and D_2 were both larger than the expected diffusion coefficient for monomer lipid by several orders of magnitude, had large standard errors, and are probably statistically meaningless. Constraining D_1 and D_2 to expected values of diffusion constants for vesicles and monomer lipid resulted in very poor fits to the data. For both sets of data, fitted values of Γ_m and K_1 were similar to those determined from the one-component model. For the higher concentrations, calculated values for K_2 were >1 and had large standard errors.

The data for the lower vesicle concentrations were also fit with the two-component version of Eq. (7), the model that corresponds to the kinetic limit associated with surface reorganization. Again, these data sets were fit simultaneously to

reduce degeneracy in the fit. Fitted values for Γ_m and K are approximately the same as those received by fitting the data to the one-component model at the kinetic limit. The reorganization rate constant that would correspond to a putative second component species was calculated to be two orders of magnitude larger than the rate constant calculated for reorganization of vesicles. The explicit consideration of a contribution from monomer lipid did not in any case provide a significantly better fit to the data than did the consideration of a single component.

3.4. Cell membrane hybrid layers

The addition of red blood cell ghosts to the alkanethiol monolayer resulted in the addition of cell membrane lipid, protein and carbohydrate components to the surface [9]. The RBC ghosts appear to interact with and reorganize at the hydrophobic surface in a manner that is analogous to that of phospholipid vesicles resulting in a bilayer that consists of an alkanethiol monolayer plus additional material that is equivalent in thickness to approximately one half of a cell membrane.

The kinetics of the reaction between RBC ghosts and the alkanethiol monolayer in non-flowing conditions (Fig. 4) differ from those seen for phospholipid vesicles in two ways. First, the formation of the bilayer is slower. In addition, the ghosts tend to result in weakly associated multilayers at the surface under non-flowing conditions. The hydrodynamic radius of RBC ghosts was measured to be 1.58 μm by quasi-elastic light scattering. RBC ghosts are much larger than phospholipid vesicles and diffuse much more slowly. Based on the observations with phospholipid vesicles, we might expect that the small diffusion coefficient associated with RBC ghosts would result in a large value for K^2/D, and that RBC ghost hybrid bilayer formation would be diffusion dependent. As shown in Fig. 4, the data were fit very well to Eq. (6), the diffusion-dominated limit. For the fit shown in Fig. 4, the calculated value for Γ_m was significantly larger

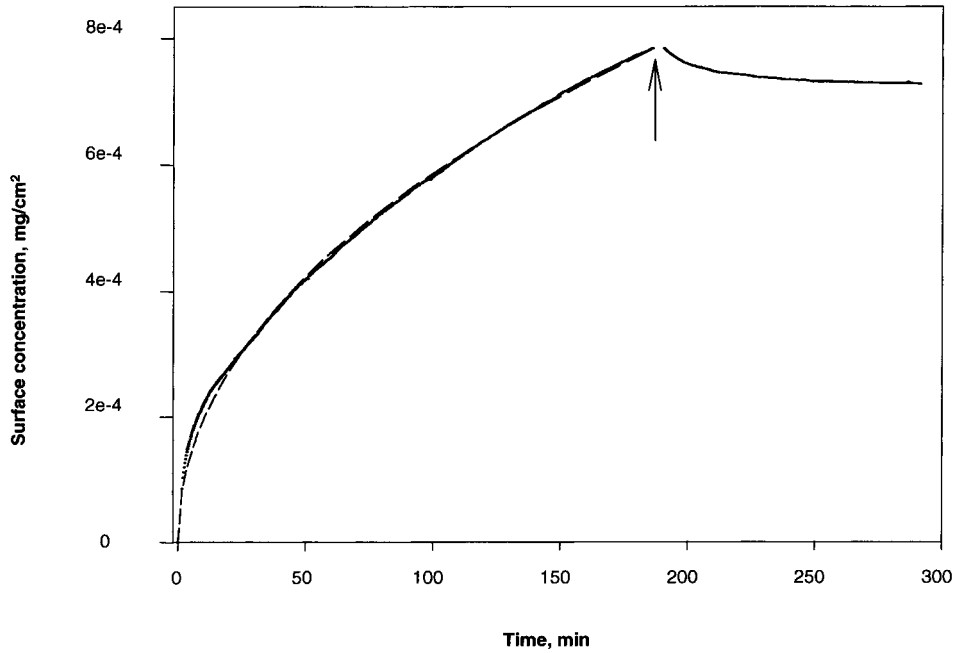

Fig. 4. Formation of a hybrid bilayer by addition of ghosts of red blood cell ghosts, at time 0, to the hydrophobic alkanethiol surface. The dashed line is calculated using Eq. (6), the diffusion limited case. The arrow marks the time at which ghosts were removed from the cell, and the solution was replaced with buffer.

than values calculated for vesicles, reflecting the formation of multilayers. The diffusion coefficient, D, was kept constant at its measured value, but C_0 was allowed to float. The fitted value for C_0 was 0.16 mg ml^{-1}, which compares well with the estimated concentration of cell membrane lipid and protein in the solution.

4. Conclusions

The kinetic analysis presented here shows that the rate of bilayer formation by the rearrangement of phospholipid vesicles or red blood cell ghosts at a hydrophobic surface is dependent on the lipid concentration, and, at high concentrations, on the diffusion constant of the vesicles or ghosts. Our data indicate that the formation of a bilayer appears to be a vesicle-dependent process that is not strongly contributed to by phospholipid monomers directly. The apparent unimportance of phospholipid monomer in the addition of lipid to the surface may reflect that vesicles contribute much more to covering surface area per 'event' than do individual lipid molecules.

At high concentrations of lipid vesicles or RBC ghosts, the rate of bilayer formation can be attributed solely to diffusion of vesicles or ghosts. The diffusion coefficients corresponding to the fits for these data are reasonable estimates of their measured diffusion coefficients, even though the diffusion coefficients for vesicles and ghosts are very different.

A significant practical implication of this work is that more efficient monolayer formation occurs at higher vesicle concentrations. At low concentrations of vesicles, formation of the bilayer is clearly not mass transport limited. Instead, the rate-limiting step appears to be a kinetic process at the surface that results in the system behaving like a partially reflecting boundary to vesicles. These results have interesting implications for the details of bilayer formation, even in the high concentration regime, despite the apparent straightforward kinetic analysis in this regime. Apparently, the concentration of vesicles at the surface influences the rate of reorganization. At higher concentrations, reorganization of vesicles at the surfaces is rapid enough to cause depletion of vesicles near the surface, resulting in the appearance of diffusion of vesicles as the rate-limiting step. This suggests the possibility of a catalytic effect of neighboring vesicles or their component phospholipids on the hybrid bilayer, since at low concentration of vesicles, diffusion of vesicles is not an important kinetic parameter.

Our observation of a surface reorganization kinetic process, characterized by K, which is only significant at low concentrations of vesicles, indicates that the surface reaction is not as simple as we have envisioned it for this analysis. Dependence of the kinetics of surface reorganization on the bulk concentration of vesicles would not be consistent with our boundary condition, which implies pseudo-first-order kinetics. The uncertainty and complexity of introducing a more specific surface reorganization process justifies this initial approach to understanding the kinetics of bilayer formation.

The driving force for bilayer formation clearly is the free energy of the hydrophobic surface in contact with water. But the activation energy barrier associated with the de-lamination or other destabilization of the lipid vesicle, a thermodynamically stable structure, must be substantial. A recent report [5] demonstrates different rates of bilayer formation when egg phospholipid vesicles are added to hydrophobic monolayers of octadecanethiol, or hydrophilic monolayers of ethylenoxythiol, or monolayers containing different amounts of a cholesterol functionalized thiol derivative. Single layers of phospholipid were added to the hydrophobic octadecanethiol or 100% cholesterol functionalized thiol layers, while both leaflets of a phospholipid vesicle bilayer added to the hydrophilic surfaces. Those comparative data demonstrated that addition of a monolayer of phospholipid to a hydrophobic surface is the slower process, suggesting, as our data do, that a rate-determining step other than diffusion to the surface is involved.

Comparison of our data with the kinetic study of Kalb [1] on bilayers formed by addition of vesicles to transferred phospholipid Langmuir Blodgett films indicates some similarities and some differences between these systems. The kinetics of formation are similar. All experiments

for this study were performed in buffered aqueous solution, but at low ionic strength. Kalb et al. showed data indicating the failure to form a bilayer in low salt concentration [1]. This may simply reflect the special solution requirements of their system for maintaining the weak interactions between the lipid headgroups and the glass support. An advantage associated with the use of alkanethiols on gold is the completeness of the layer formed and its stability over time and under different experimental conditions.

In the protein adsorption literature it is common practice to fit experimental adsorption profiles with some linear combination of Eq. (6) and Eq. (7), with the implicit assumption that the various processes are independent of one another [14]. However, this additivity assumption cannot be valid unless the absorbing and reflecting patches of the surface are simply connected mesoscopically large regions. The reason for this is that the perfectly absorbing portions of the surface give rise to a concentration depletion zone in the vicinity of the surface that extends well into the reflecting regions. Therefore, such a surface will generally appear to be a good deal more absorbing than would be implied by a simple geometric partitioning into absorbing and reflecting patches. There are also examples of treating adsorption profiles with a stretched exponential representation, with a temperature dependent index which is allowed to range from $1/2$ to unity [15]. We have found that the complete expression given by Eq. (1) provides a more satisfactory description of the data. In addition, it is mathematically exact and has a meaningful physical interpretation.

Acknowledgements

The authors would like to thank Dr. J. Given of C.A.R.B. for his assistance in mathematical modeling.

References

[1] E. Kalb, S. Frey, L.K. Tamm, Formation of supported planar bilayers by fusion of vesicles to supported phospholipid monolayers. Biochim. Biophys. Acta 1103 (1992) 307–316.

[2] A.L. Plant, M. Guegeutchkeri, W. Yap, Supported phospholipid/alkanethiol biomimetic membranes: insulating properties. Biophys. J. 67 (1994) 1126–1133.

[3] C.W. Muese, G. Niaura, M.L. Lewis, A.L. Plant, Assessing the molecular structure of alkanethiols in supported hybrid bilayer membranes with vibrational spectroscopy. Langmuir 14 (1998) 1604–1611.

[4] C.W. Meuse, S. Krueger, C.F. Majkrzak, J.A. Dura, J. Fu, J.T. Conner, A.L. Plant, Hybrid bilayer membranes in air and water: infrared spectroscopy and neutron reflectivity studies. Biophys. J. 74 (1998) 1388–1398.

[5] L.M. Williams, S.D. Evans, T.M. Flynn, A. Marsh, P.F. Knowles, R.J. Bushby, N. Boden, Kinetics of the unrolling of small unilamellar phospholipid vesicles onto self-assembled monolayers. Langmuir 13 (1997) 751–757.

[6] H. Lang, C. Duschl, H. Vogel, A new class of thiolipids for the attachment of lipid bilayers on gold surfaces. Langmuir 10 (1994) 197–210.

[7] S. Lingler, I. Rubinstein, W. Knoll, A. Offenhausser, Fusion of small unilamellar lipid vesicles to alkanethiol and thiolipid self-assembled monolayers on gold. Langmuir 13 (1997) 7085–7091.

[8] B.J. Berne, R. Pecora, Dynamic Light Scattering, John Wiley, New York, 1976, pp. 59–60.

[9] N.M. Rao, A.L. Plant, V. Silin, S. Wight, S.W. Hui, Characterization of biomimetic surfaces formed from cell membranes. Biophys. J. 73 (1997) 3066–3077.

[10] T.L. Steck, J.A. Kant, Preparation of impermeable ghosts and inside-out vesicles from human erythrocyte membranes. Methods Enyzmol. 31 (1974) 172–180.

[11] S.A. Rosenberg, G. Guidotti, The proteins of the erythrocyte membrane: structure and arrangement in the membrane, in: G.A. Jamieson, T.J. Greenwalt (Eds.), The Red Cell Membrane, J.B. Lippencott, Philadelphia, 1969, pp. 93–109.

[12] V. Silin, A. Plant, Biotechnological applications of surface plasmon resonance. TIBTECH 15 (1997) 353–359.

[13] V. Silin, H. Weetall, D.J. Vanderah, SPR studies of nonspecific adsorption kinetics of human IgG and BSA on gold surfaces modified by self-assembled monolayers. J. Colloid Interface Sci. 185 (1997) 94–103.

[14] R. Kurrat, J.J. Ramsden, J.E. Prenosil, Kinetic model for serum albumin adsorption: experimental verification. J. Chem. Soc. Faraday Trans. 90 (1994) 587–590.

[15] J.F. Douglas, P. Frantz, H.E. Johnson, H. Schneider, S. Granick, Regimes of polymer adsorption–desorption kinetics. Colloids Surf. A 86 (1994) 251–254.

[16] M. Abramowitz, I.A. Stegun, Handbook of Mathematical Functions, National Bureau of Standards Applied Mathematics Series 55, US Government Printing Office, 1966, chapter 7.

[17] H.S. Carslaw, J.C. Jaeger, Conduction of Heat in Solids, 2nd ed., Oxford, 1989, Sec. 2.7.

[18] J.F. Douglas, H.E. Johnson, S. Granick, A simple kinetic model of polymer adsorption and desorption. Science 262 (1993) 2010–2012.

[19] J.D. Andrade, V. Hlady, Adv. Polymer Sci. 79 (1986) 3–56.
[20] W. Norde, Adv. Colloid Interface Sci. 25 (1986) 276–340.
[21] D. Marsh, CRC Handbook of Lipid Bilayers, CRC Press, Boca Raton, 1990.
[22] M.J. Janiak, D.M. Small, G.G. Shipley, J. Biol. Chem. 254 (1976) 6068.
[23] R. Smith, C. Tanford, The critical micelle concentration of L-α-dipalmitoylphosphatidylcholine in water and water/methanol solutions. J. Mol. Biol. 67 (1972) 75–83.
[24] H.J. Pownall, L.M. Diane, J.B. Massey, Spontaneous phospholipid transfer: development of a quantitative model. Biochemistry 30 (1991) 5696–5700.